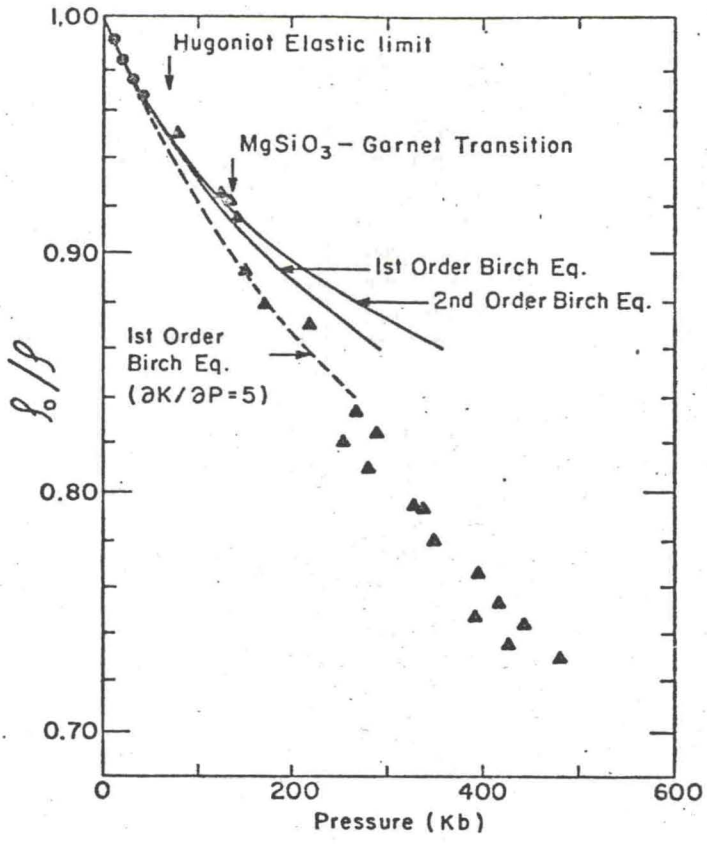


Fig. 7. Comparison of ultrasonic equation of state for bronzite calculated from Birch's equations with static-compression data of *Bridgman* [1948] (circles) and shock-wave data of *Ahrens and Gaffney* [1971] (triangles and dashed lines).

range of the orthopyroxene structure extends to higher pressures, say, to about 200–300 kb, or if the nonlinearity of the on-diagonal longitudinal constants turns out to be very large.

In addition to the acoustic measurements of this study, isothermal-compression data on hypersthene to 40 kb [*Bridgman*, 1948] and shock-compression data on Bamle enstatite [*Ahrens and Gaffney*, 1971] have been included in Figure 7 for comparisoin. Although a direct comparison with the present data is not possible because the shock data are not isothermal, it is worthy to note that the three shock points between the Hugoniot elastic limit, where enstatite should behave plastically, and approximately 150 kb are in reasonable agreement with the present data. Further examination of the shock data in the 150-kb regions shows a discontinuity indicative of a possible phase transition. By constructing an enstatite isentrope with *Kumazawa's* [1969] value of the adiabatic bulk modulus and an assumed low pressure derivative of 5.0, *Ahrens and Gaffney* [1971] argued that the final Hugoniot states above a level of approximately 135 kb lie at a greater density than that indicated for the enstatite isentrope. By converting their values used for calculating the enstatite isentrope to isothermal quantities, the extrapolated curve also shown in Figure 7 was obtained. However, when the present data are compared with the shock-compression values, the discontinuity is more convincingly illustrated, and thus the interpretation of a phase transition in the vicinity of 135 kb is supported.

*Pressure dependence of lattice parameters.* *Thurston* [1967] has proposed an equation of state that permits the calculation of the lattice parameters $a_i$ ( $i = 1, 2, 3$) as a function of pressure from the principal stretches $\lambda_i$ according to

$$\lambda_i = \frac{a_i(P)}{a_i^0} = \left[1 + \left(\frac{\partial K^T}{\partial P}\right)_T \frac{P}{K^T}\right]^{m_i} e^{n_i P} \quad (12)$$

$$i = 1, 2, 3$$

The index 0 refers to zero pressure. The parameters $m_i$ and $n_i$ depend on the isothermal elastic compliances and the isothermal pressure derivatives of the isothermal effective elastic constants according to (I, 88), (I, 90), (II, 9), and (II, 15) of *Thurston* [1967]. Their numerical values as calculated from the experimental data of Tables 6 and 7 are listed in Table 14. Also included in this table are the zero pressure lattice parameters $a_i^0$ as determined from X-ray measurements in this laboratory [*Frisillo and Buljan*, 1972] (these values agree quite closely with those reported by *Wyckoff* [1968] for $Mg_{0.465}Fe_{0.535}SiO_3$, namely, $a_0 = 18.310$ A, $b_0 = 8.927$ A, and $c_0 = 5.226$ A) and the linear compressibilities $\alpha_i = (\partial \ln a_i/\partial P)_T$ and their pressure coefficients $\beta_i = (\partial \alpha_i/\partial P)_T$ as calculated from the data of Tables 6 and 7 on the basis of (I, 88) and (I, 90) of *Thurston* [1967]. In Figure 8 the principal stretches and the lattice parameters as calculated from (12) are plotted as a function of pressure. No directly measured data are available for comparison.

Although Thurston's equation of state (12) is a generalization of Murnaghan's equation of state and is therefore based on the linear approximation for the elastic constant versus pressure relation, its range of validity may be more limited because it is based on equation (II, 10) of *Thurston* [1967] as an additional assumption. Although Thurston's equation has been verified for several materials up to pressures of about 30% of the bulk modulus [*Thurston*, 1967] and for $Al_2O_3$ up to pressures of 10% of the bulk modulus [*Gieske and Barsch*, 1968], discrepancies have been reported for $Mg_2SiO_4$ (forsterite) [*Olinger and Duba*, 1971]. Apart from such experimental errors in the high-pressure X-ray data of *Olinger and Duba* [1971] as may result from nonhydrostatic stresses in their opposed anvil system, the possibility cannot be ruled out that the discrepancies arise from the fact that equation (II, 10) of *Thurston* [1967] does not hold for forsterite. For this reason the pressure dependence of the lattice parameters (Figure 8) should be considered as a plausible prediction only, until Thurston's equation (12) is tested for a larger variety of materials. Additional errors may arise from neglecting the quadratic terms in the pressure dependence of the elastic constants and from using the isothermal pressure derivatives of the adiabatic elastic constants (Table 7) instead of the unknown isothermal pressure derivatives of the isothermal elastic constants. Both errors, however, may be expected to be small.

With these reservations about the dependability of Thurston's equation (12) in mind, one can conclude from Figure 8 that the compression behavior of the three orthorhombic axes is noticeably different. Especially noteworthy is the rapid decrease of the slope of the curve for the $c$ axis, which indicates a rapid decrease of the linear compressibility in this direction. At 200 kb, for example, the linear compressibility of the $c$ axis is 3 and 6 times smaller than the linear compressibilities of the $a$ and $b$ axes, respectively. Undoubtedly, this behavior arises from the special features of the crystal structure of enstatite. This structure consists of $SiO_4$ chains extending along the $c$ direction and interconnected by the (Mg, Fe) cations [*Wyckoff*, 1968]. Thus, although the initial linear compressibilities along the different crystallographic

TABLE 14. Zero Pressure Lattice Parameters $a_i^0$, Linear Compressibilities $\alpha_i$, Pressure Coefficients $\beta_i$, and Exponents $m_i$ and $n_i$ of Thurston's Equation of State

| Axis | $i$ | $a_i^0$, A | $\alpha_i$, $Mb^{-1}$ | $\beta_i$, $Mb^{-2}$ | $m_i$ | $n_i$, $Mb^{-1}$ |
|---|---|---|---|---|---|---|
| $a$ | 1 | 18.262 | -0.2344 | 1.858 | -0.02000 | -0.04448 |
| $b$ | 2 | 8.870 | -0.4375 | 3:603 | -0.03783 | -0.07828 |
| $c$ | 3 | 5.203 | -0.3303 | 4.411 | -0.04771 | 0.12276 |